A)

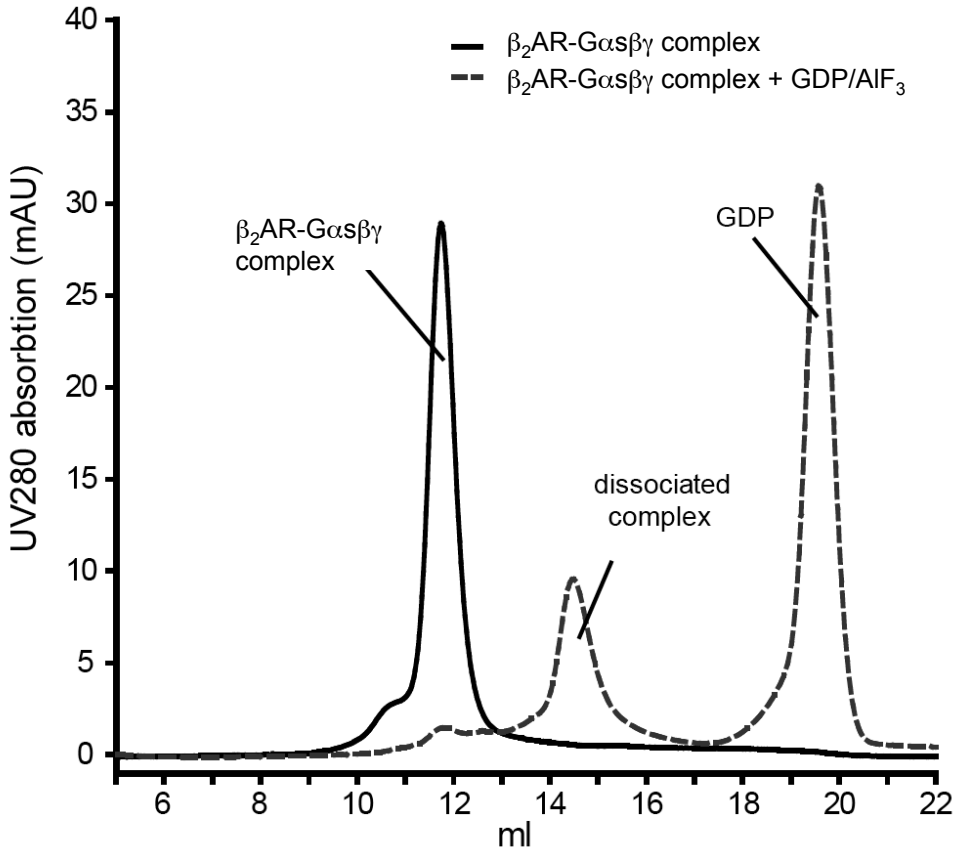
β2AR-Gαsβγ complex
β2AR-Gαsβγ complex + GDP/AlF3
UV280 absorbtion (mAU)
40
35
30
25
20
15
10
5
0
β2AR-Gαsβγ complex
GDP
dissociated complex
6
8
10
12
14
16
18
20
22
ml

B)

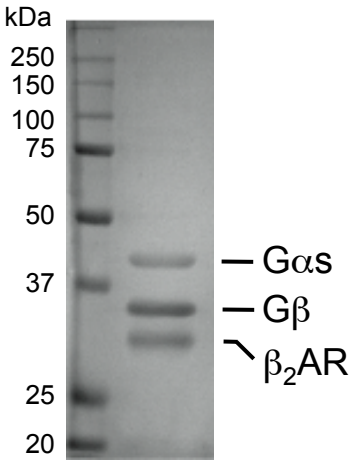
kDa
250
150
100
75
50
37
25
20
Gαs
Gβ
β2AR

Figure S1

Supplemental Figure Legends

Figure S1

Analysis of the purity and integrity of the β_2AR-Gs complex by size exclusion chromatography. A) Purified β_2AR-Gs complex was applied to a Superdex 200 (HR10/30, GE Healthcare, Piscataway, NJ) column (black) following pre-incubation in a presence (dotted) or absence (solid) of GDP/AlF_3. The disappearance of the elution peak (containing the β_2AR-Gs complex) at ~12.8 ml by uncoupling with GDP/AlF_3 indicates that the G protein is active and functional. The β_2AR-Gs complex was detected by UV absorption. B) Silver stain of the purified β_2AR-Gs complex resolved by SDS-PAGE following M1-Flag affinity and size exclusion column chromatography.

DXMS in Gαs

A) Gαsβγ

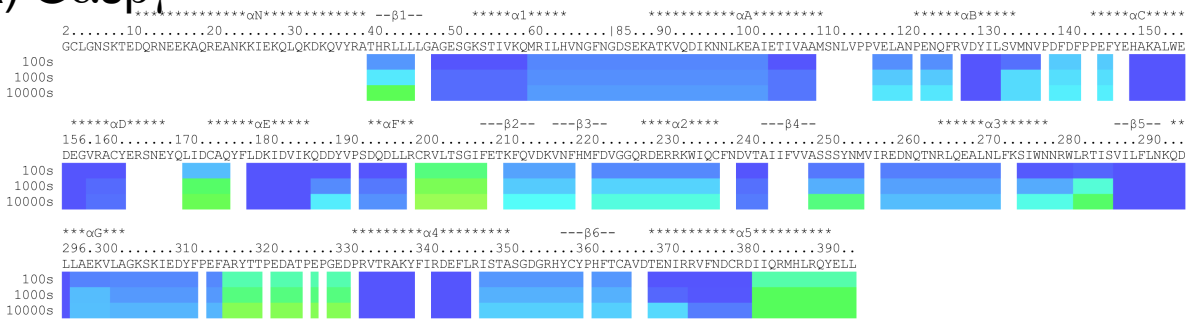

B) β_2AR-Gαsβγ complex

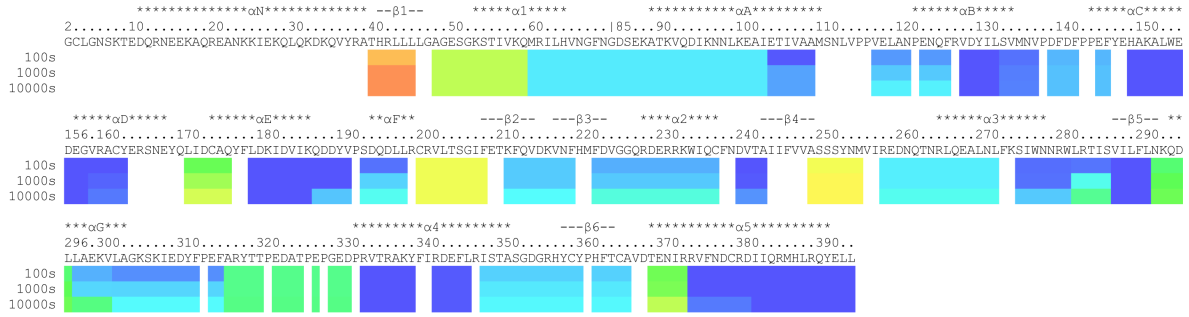

C) β_2AR-Gαsβγ complex + GDP/AlF_3

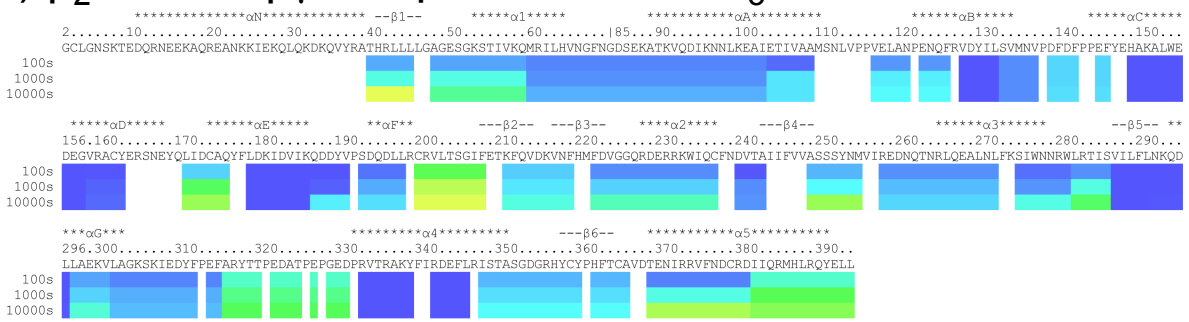

D) β_2AR-Gαsβγ complex + GDP

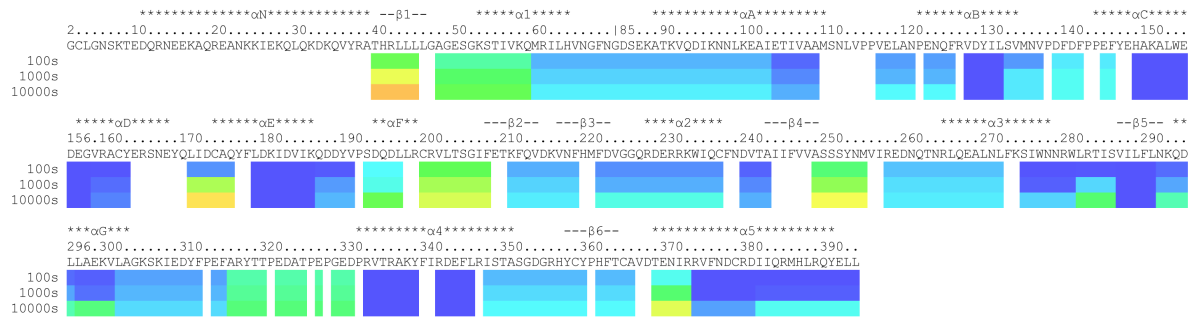

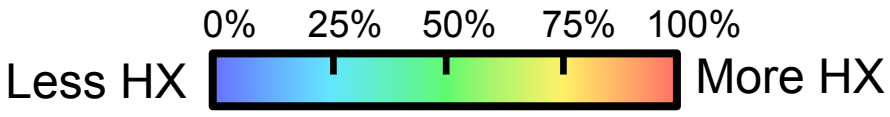

Figure S2

Figure S2

Ribbon diagram of the hydrogen-deuterium exchange levels of Gαs in heterotrimer alone (A) or in complex with the β_2AR (B). Exchange levels were also assessed in the complex treated with GDP/AlF_3 (C) or with GDP alone (D). Indicated is the amino-acid sequence and secondary structure. Exchange levels were color-coded according to the indicated heat map. Residues not coloured represent fragments where no mass information was obtained.

DXMS in Gβ and Gγ

A) Gαsβγ

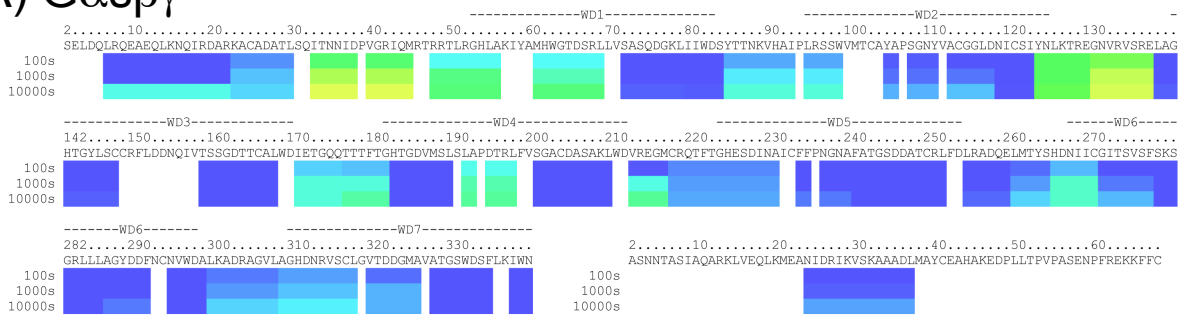

B) β_2AR-Gαsβγ complex

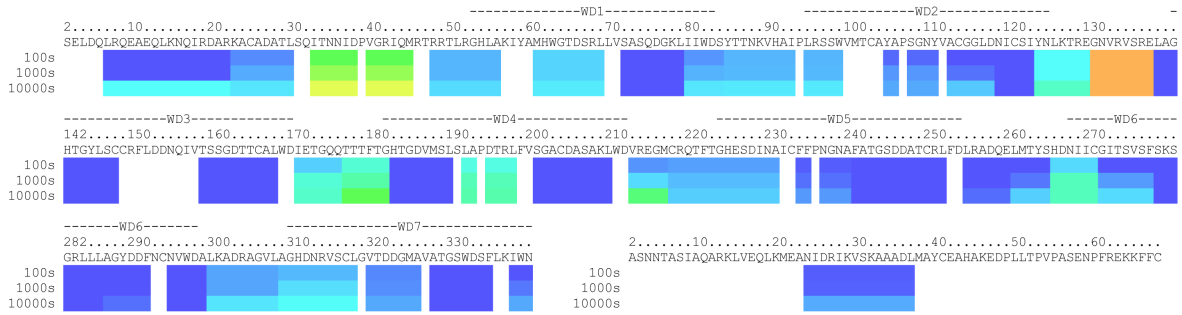

C) β_2AR-Gαsβγ complex + GDP/AlF_3

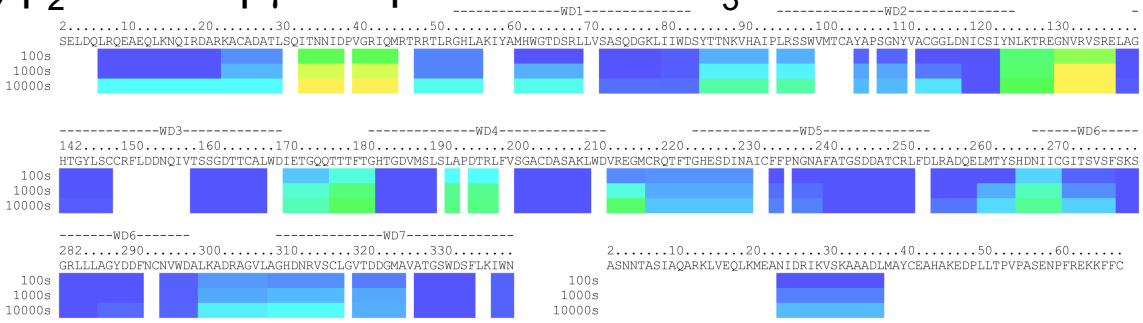

D) β_2AR-Gαsβγ complex + GDP

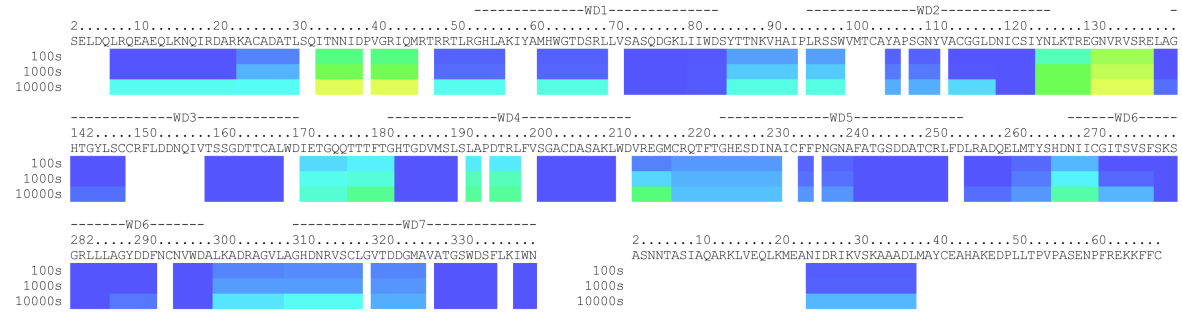

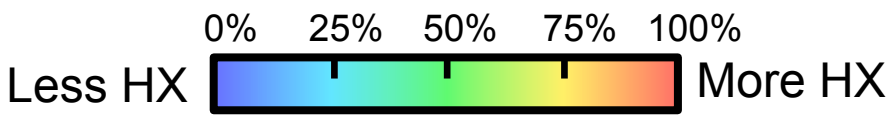

Figure S3

Figure S3

Ribbon diagram of the hydrogen-deuterium exchange levels of Gβ and Gγ in heterotrimer alone (A) or in complex with the β_2AR (B). Exchange levels were also assessed in the complex treated with GDP/AlF_3 (C) or with GDP alone (D). Indicated is the amino-acid sequence and secondary structure. Exchange levels were colour-coded according to the indicated heat map. Residues not coloured represent fragments where no mass information was obtained.

DXMS in β_2AR

A) β_2AR-Gαs$\beta\gamma$ complex

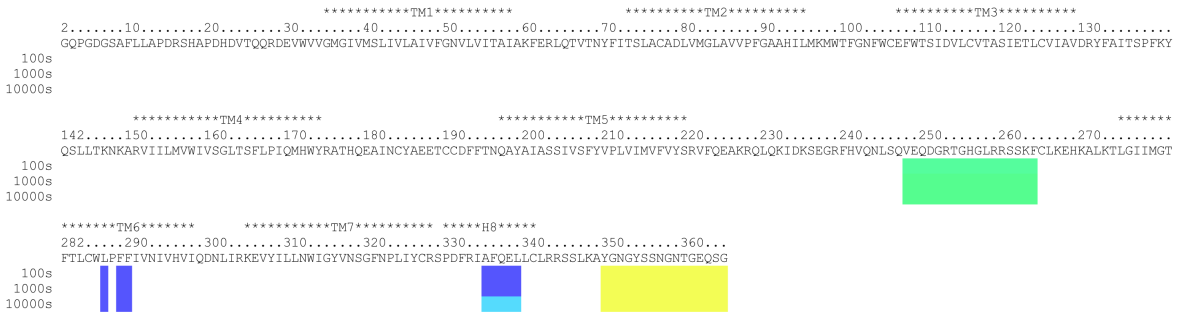

B) β_2AR-Gαs$\beta\gamma$ complex + GDP/AlF$_3$

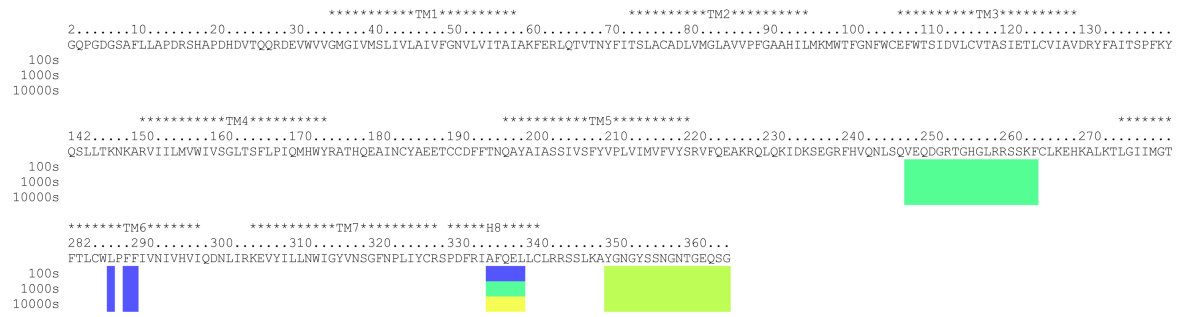

C) β_2AR-Gαs$\beta\gamma$ complex + GDP

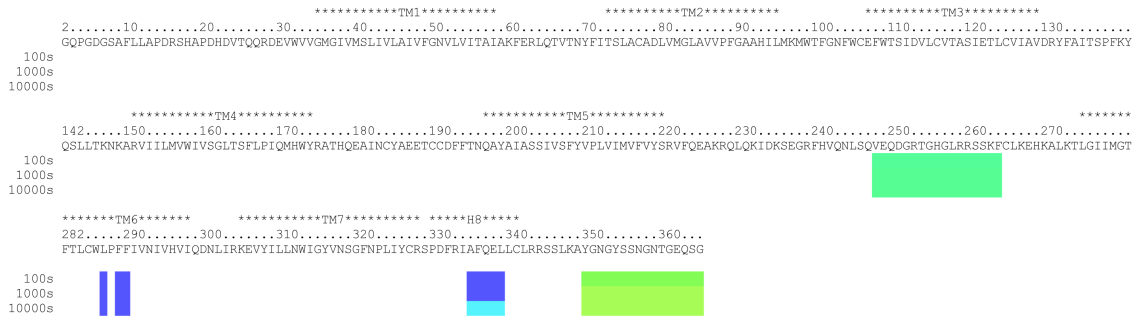

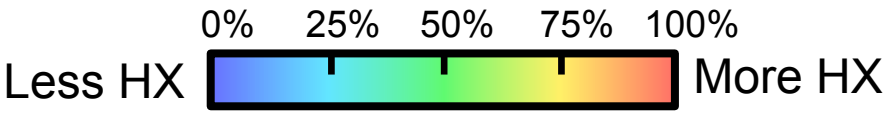

Figure S4

Figure S4

Ribbon diagram of the hydrogen-deuterium exchange levels of β_2AR in a complex with the Gαs$\beta\gamma$ heterotrimer in the absence (A) or presence of GDP/ AlF_3 (B) or with GDP alone (C). Indicated is the amino-acid sequence and secondary structure. Exchange levels were colour-coded according to the indicated heat map. Residues not coloured represent fragments where no mass information was obtained.

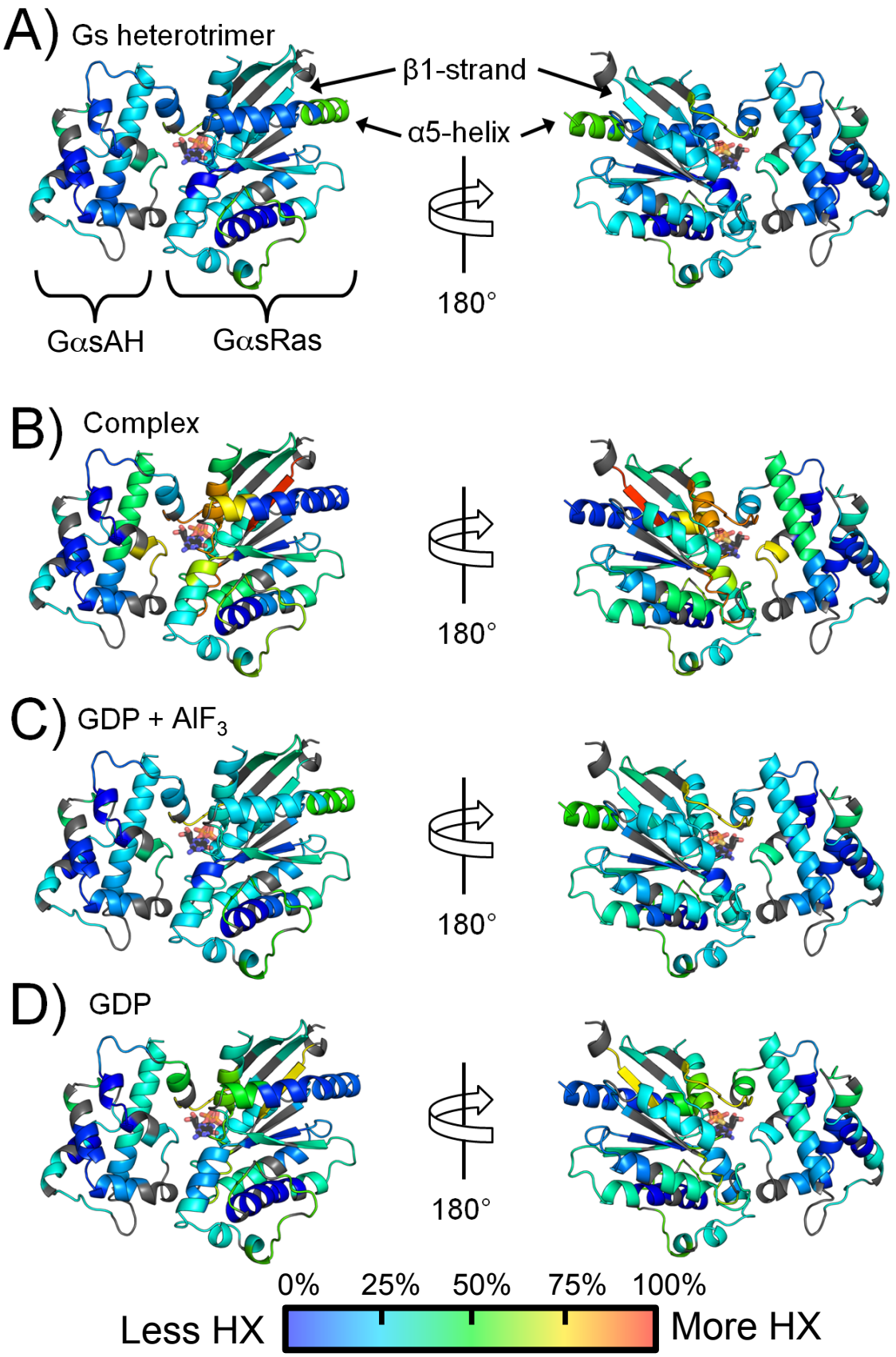
A) Gs heterotrimer
β1-strand
α5-helix
180°
GαsAH
GαsRas
B) Complex
180°
C) GDP + AlF3
180°
D) GDP
180°
0%
25%
50%
75%
100%
Less HX
More HX

Figure S5

Figure S5

Deuterium exchange levels of Gαs (from data in Fig S2A) in the heterotrimer alone (A) or in complex with the β_2AR (B) or as a complex treated with GDP/AlF_3 (C) or with GDP alone (D). Deuterium exchange levels following incubation with deuterium for 100 s at 4C mapped on to the structure of Gαs in its GTPγS-bound form (PDB: 1AZT)[6]. Indicated are the ras and helical domain. The β1-strand and α5-helix, two regions displaying major changes in deuterium exchange are also indicated. Exchange levels were colour-coded according to the indicated heat map. Residues coloured gray represent fragments where no mass information was obtained.

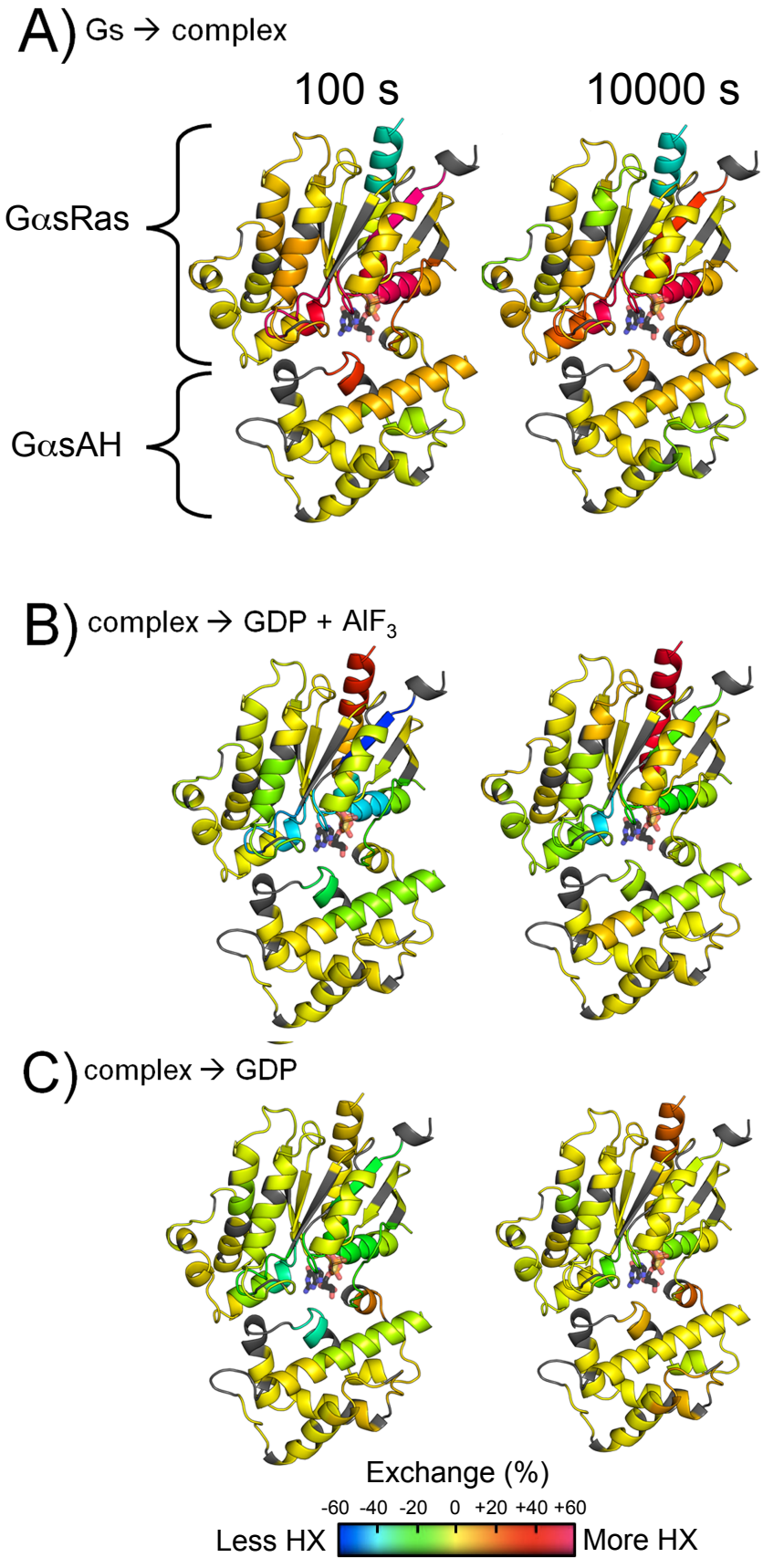
A) Gs → complex
100 s
10000 s
GαsRas
GαsAH
B) complex → GDP + AlF3
C) complex → GDP
Exchange (%)
-60 -40 -20 0 +20 +40 +60
Less HX
More HX

Figure S6

Figure S6

DXMS reveals conformational changes in the Gαs when in complex with agonist-bound β_2AR in solution. Comparative DXMS analysis, of heterotrimer Gαsβγ when interacting with agonist (BI-167107)-bound β_2AR (A), when uncoupled with the addition of GDP/AlF_3 (B), or with the addition of GDP alone (C). The changes in amide hydrogen-deuterium exchange, given as changes in the percentage of the theoretical maximum number of deuterons incorporated per peptide, were mapped on to the crystal structure of Gαs based on the GTPγS-bound form (PDB:1AZT). Residues displaying increases (red) and decreases (blue) in deuterium incorporation during the transitions were plotted according to the indicated heat map. Regions that are not covered are indicated in gray. Among 3 time points analyzed (Figure 2S), 100 and 10,000 sec time points are presented

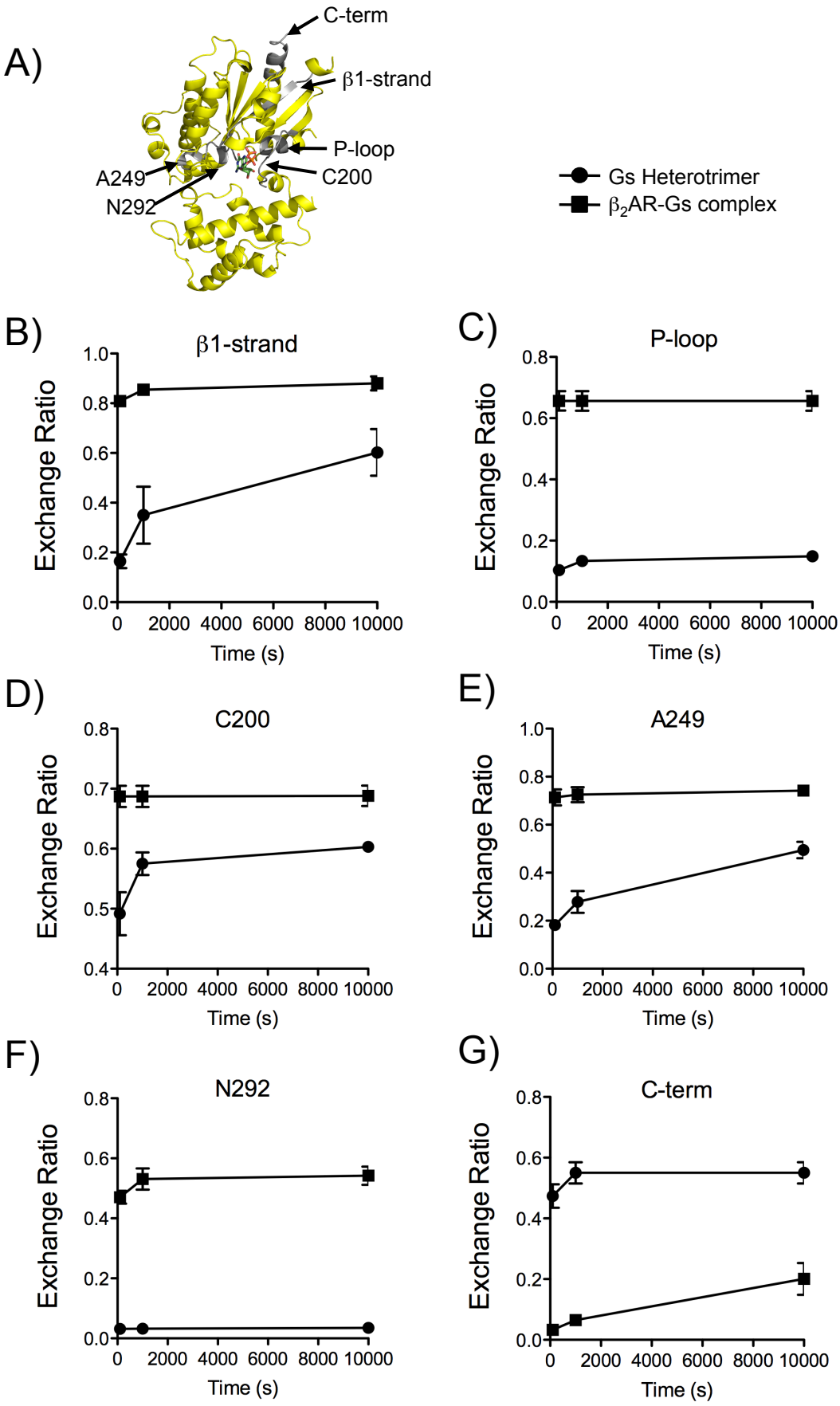
A)
C-term
β1-strand
P-loop
A249
C200
N292
Gs Heterotrimer
β2AR-Gs complex
B)
β1-strand
C)
P-loop
D)
C200
E)
A249
F)
N292
G)
C-term
Exchange Ratio
Time (s)
0
2000
4000
6000
8000
10000

Figure S7

Figure S7

Time course of deuterium-hydrogen exchange in the Gαs subunit in the Gs heterotrimer alone (circles) or in complex with the β_2AR (squares). A) indicated in gray are regions of Gαs that display the largest changes in hydrogen-deuterium exchange following formation of the β_2AR-Gs complex. Panels B) to G) represent time courses of hydrogen-deuterium exchange following incubation with deuterium for 100, 1000, and 10000 s of the β1-strand (B), P-loop (C), peptide containing C200 (D), N249 (E) A292 (F) and the C-terminal α5-helix (G). Data are from three independent DXMS experiments.

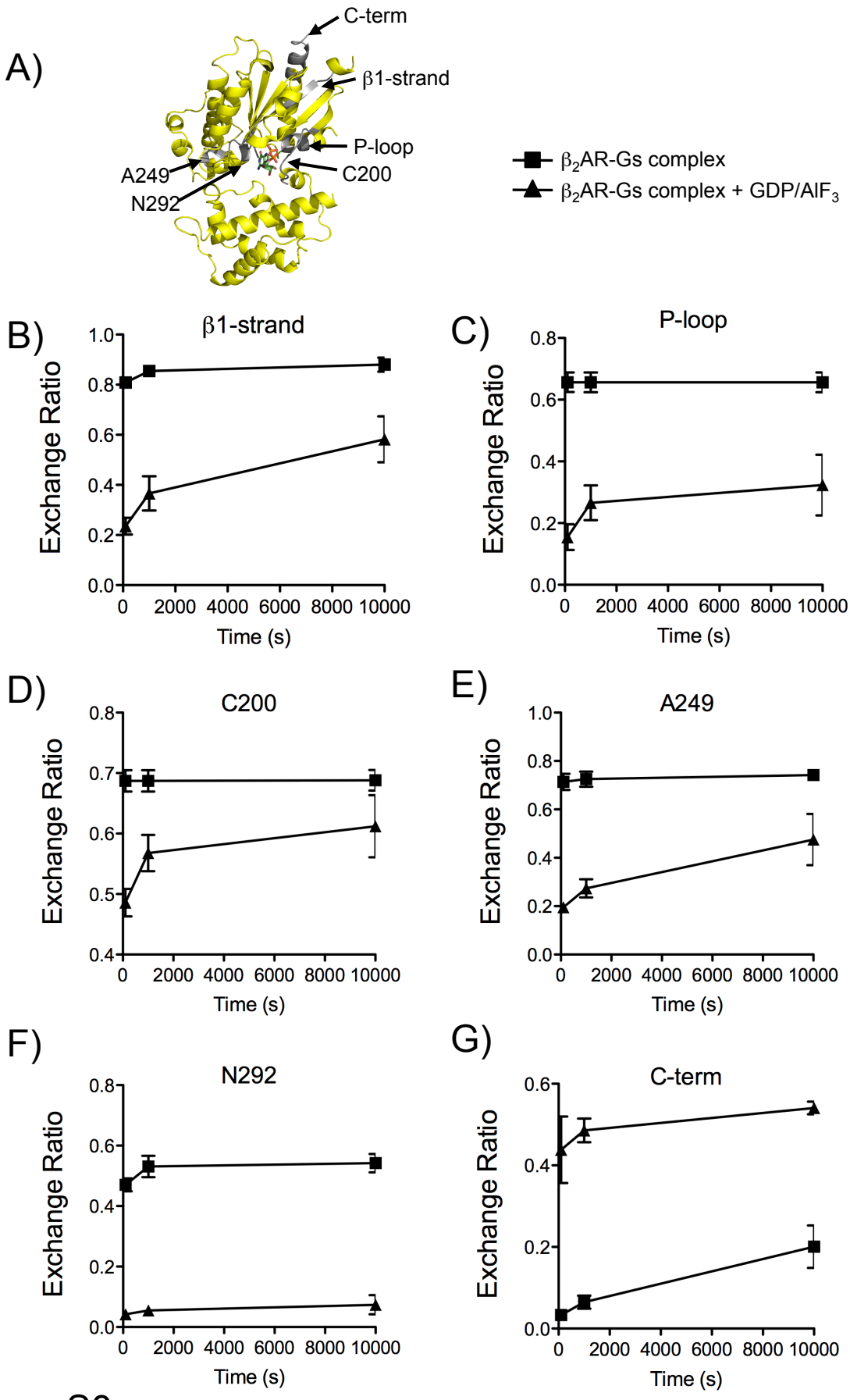
A)
C-term
β1-strand
P-loop
A249
C200
N292
β2AR-Gs complex
β2AR-Gs complex + GDP/AlF3
B)
β1-strand
C)
P-loop
D)
C200
E)
A249
F)
N292
G)
C-term
Exchange Ratio
Time (s)
0
2000
4000
6000
8000
10000

Figure S8

Figure S8

Time course of deuterium-hydrogen exchange in the Gαs subunit in the β_2AR-Gs complex in the absence (squares) or presence of GDP/AlF_3 (triangles). A) indicated in gray are regions of Gαs that display the largest changes in hydrogen-deuterium exchange following formation of the β_2AR-Gs complex. Panels B) to G) represent time courses of hydrogen-deuterium exchange following incubation with deuterium for 100, 1000, and 10000 s of the β1-strand (B), P-loop (C), peptide containing C200 (D), N249 (E) A292 (F) and the C-terminal α5-helix (G). Data are from three independent DXMS experiments.

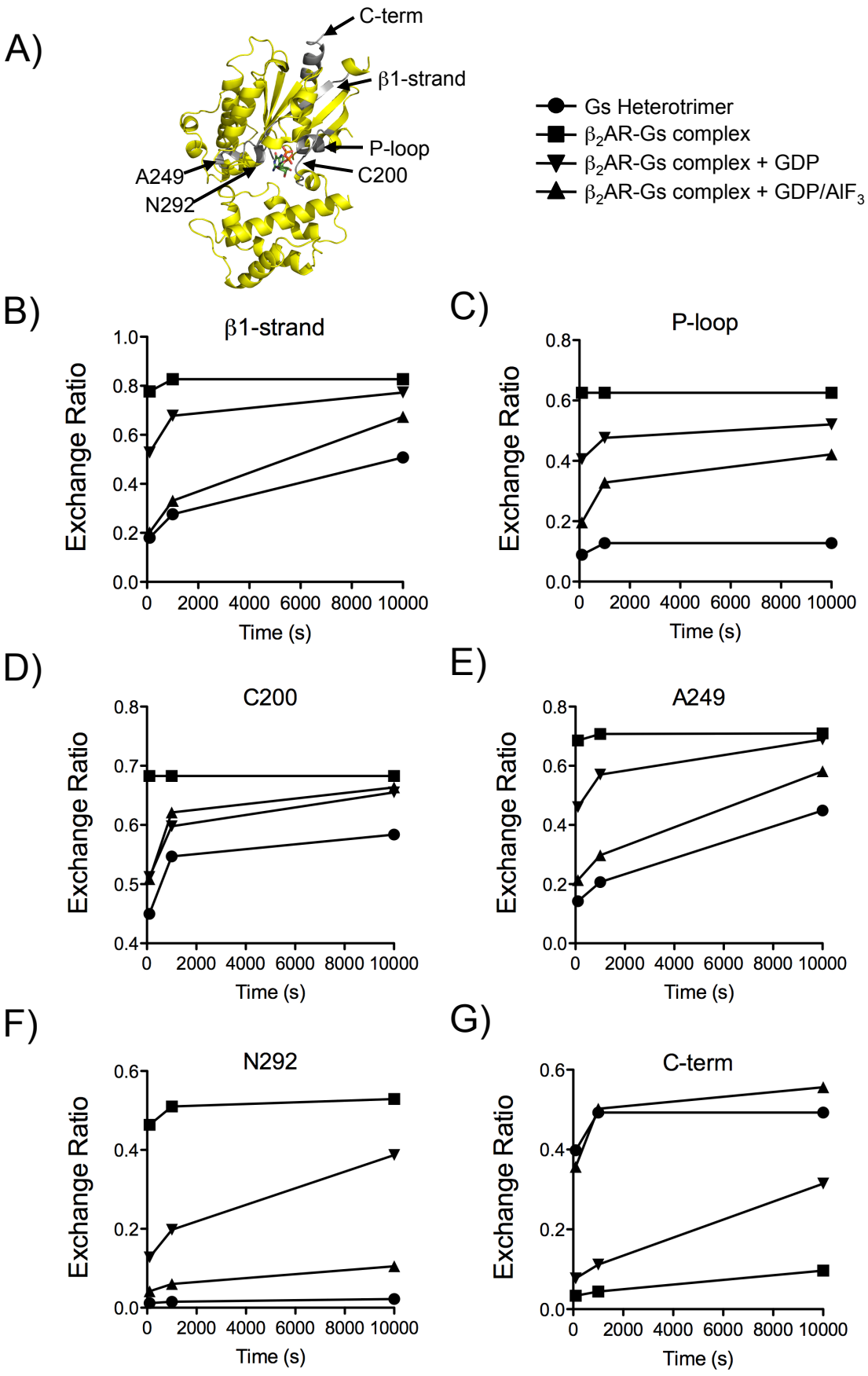
A)
C-term
β1-strand
P-loop
A249
C200
N292
Gs Heterotrimer
β2AR-Gs complex
β2AR-Gs complex + GDP
β2AR-Gs complex + GDP/AlF3
B)
β1-strand
C)
P-loop
D)
C200
E)
A249
F)
N292
G)
C-term
Exchange Ratio
Time (s)

Figure S9

Figure S9

Time course of deuterium-hydrogen exchange in the Gαs subunit in the Gs heterotrimer alone (circles), in the β_2AR-Gs complex (squares) or the complex treated with 1 mM GDP in the presence (triangles) or absence of AlF_3 (inverted triangles). A) indicated in gray are regions of Gαs that display the largest changes in hydrogen-deuterium exchange following formation of the β_2AR-Gs complex. Panels B) to G) represent time courses of hydrogen-deuterium exchange following incubation with deuterium for 100, 1000, and 10000 s of the β1-strand (B), P-loop (C), peptide containing C200 (D), N249 (E) A292 (F) and the C-terminal α5-helix (G). Data are from a single experiment where all samples were simultaneously treated and subsequently analyzed by DXMS.

A)

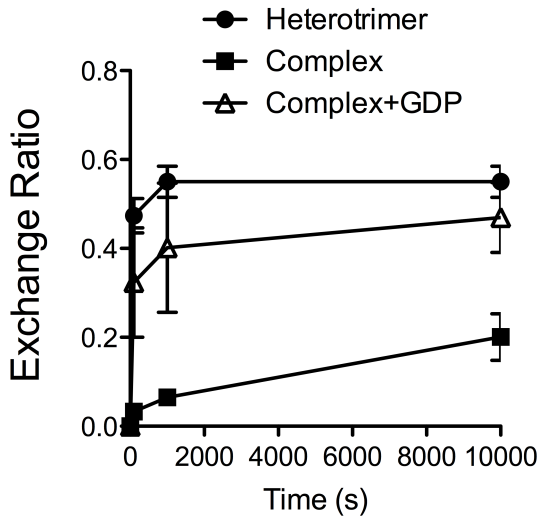

B)

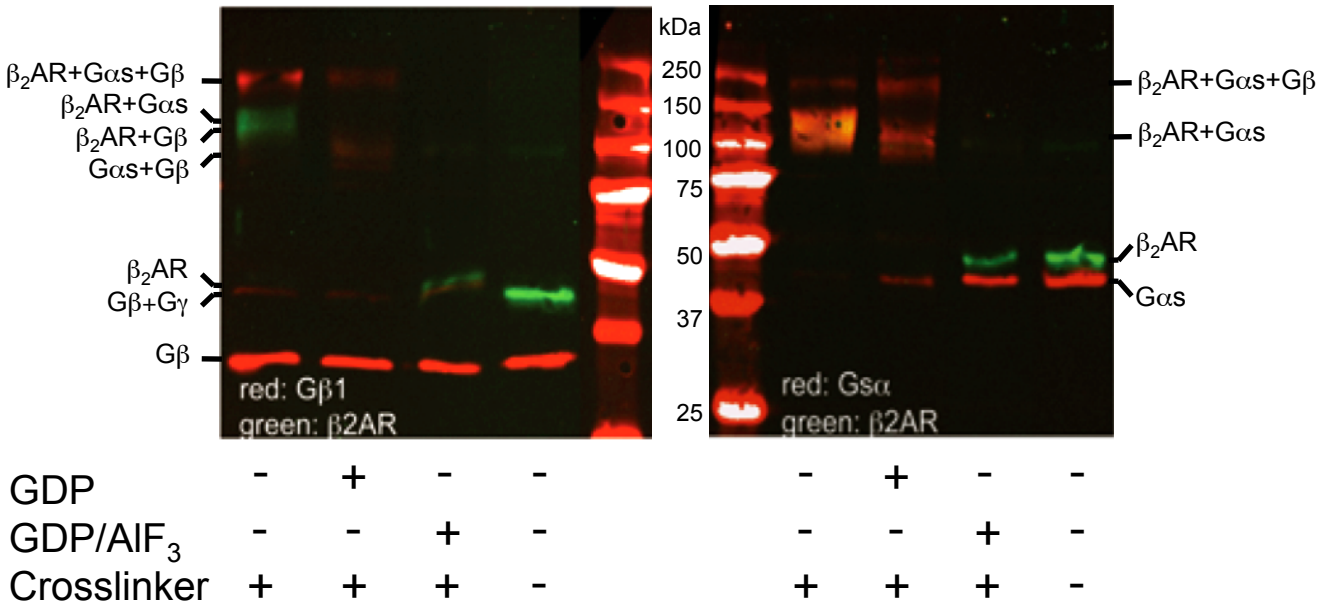

Figure S10

Figure S10

A) Time course of deuterium-hydrogen exchange in the Gαs subunit in the Gs heterotrimer alone (circles), in the β_2AR-Gs complex (squares) or the complex treated with 1 mM GDP (triangles). The GDP data shown in Figure 2 of the manuscript are compatible with a "pre-coupled" complex. The possibility that the C-terminus of Gαs can independently bind the β_2AR is supported by results presented in the crystallography paper (Figure 6, Rasmussen *et al*, published online 2011), showing that the C-terminus of Gαs when fused to the C-terminus of the β_2AR can allosterically modulate agonist binding. Nevertheless, the GDP effect on exchange in the C-terminus of the α5-helix has the highest degree of variability relative to other conditions. Moreover we have used chemical cross-linking studies to analyze the interaction between the β_2AR and Gαs and/or Gβγ in the presence or absence of GDP and/or GDP/AlF_3. Figure S10B (below) illustrates that a minor population of GDP-bound, G protein-receptor complexes may be trapped even in the presence of 1 mM GDP, but not in the presence of GDP/AlF_3.

That being said it is also well known that GDP at high concentrations have the capacity to disrupt the β_2AR-Gs complex. Thus trapping a homogenous population of GDP-bound and receptor-bound G protein complex would require just the right conditions. Taken together we feel that the existence of the GDP-bound G protein-receptor complex are supported by the DXMS analysis but that it is a weak or transient species.

The higher degree of variability in the presence of GDP is limited to this one C-terminal peptide and probably reflects the low affinity of interactions between the β_2AR and GDP bound Gs. However, because of the variability, we cannot be confident of the mechanism.

B) Trapping the β_2AR-Gs complex by crosslinking. Untreated, purified β_2AR-Gs complex or β_2AR-Gs complex treated with GDP +/- AlF_3 were crosslinked with BS2G, resolved by SDS-PAGE and analyzed for composition by western blotting.

A crosslinked complex composed of β_2AR, Gαs and Gβ is identified by western blotting with antibodies directed against each protein, in addition to stabilized complexes between β_2AR and Gαs or β_2AR and Gβ. The addition of 100 μM GDP only partially disrupted the β_2AR and Gαs or β_2AR and Gβ complexes, consistent with DXMS analysis. This is in contrast to the uncoupling effect of the addition of GDP/AlF_3, which very efficiently disrupted the complex.

β_2AR-Gs complex either treated with nucleotides (+/- 100 mM GDP) or untreated was diluted to 1 μM with buffer containing 0.0015 % MNG-3, 20 mM HEPES, pH 7.5, 100 mM NaCl, 10 μM BI-167107, and 100 μM TCEP. One μM of protein sample was crosslinked with 100 μM lysine-selective BS2G (Pierce, Rockford, IL) for 10 min at room temperature. The reaction was stopped by adding 20 mM Tris, pH 8.0, and by removing residual BS2G using Zeba^{TM} spin desalting column (Pierce, Rockford, IL). Cross-linked proteins were separated on 10% SDS-PAGE gel, and transferred to PVDF membrane for Western blotting. The membrane was blotted with commercial mouse anti-β_2AR antibody (Nouvus Biologicals, Littleton, CO), rabbit anti-Gαs specific antibody, or rabbit anti-Gβ specific antibody. IRDye800W-conjuated goat anti-mouse antibody (Rockland, Gilbertsville, PA) and IRDye700-conjugated goat anti-rabbit antibody (Rockland, Gilbertsville, PA) were used to visualize the blot with Odyssey Imager (Li-Cor, Lincoln, NE).

A. Hydrogens in N-terminus of α5

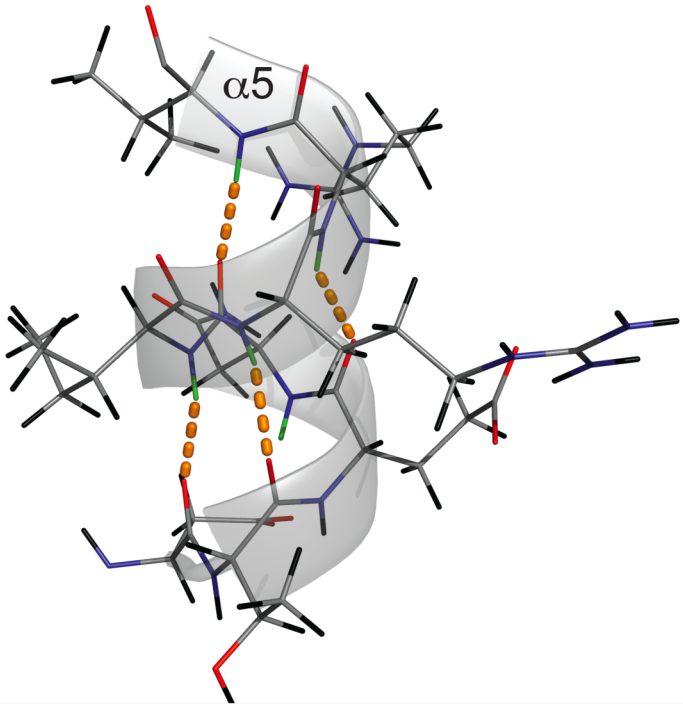

B. Hydrogens in β1

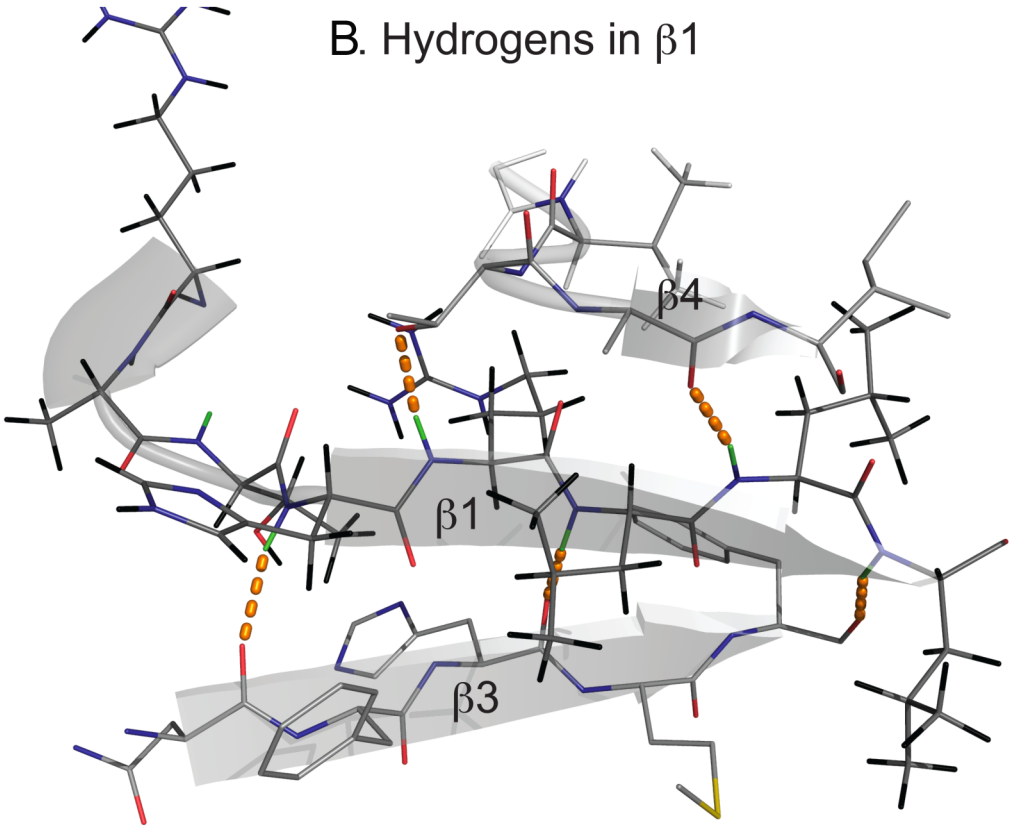

Figure S11

Figure S11

Location of the exchangeable hydrogens in the β1-strand (A) and α5-helix (B) of Gαs in its GTPγS-bound form. Residues are colour-coded as follows: Gray-carbon, Red-oxygen, Blue-nitrogen, Black-hydrogen for either slow-exchangeable or fast-exchangeable (too fast that they cannot be detected by the DXMS conditions employed). The Green-hydrogens in the amide backbone are involved in hydrogen bonds, which can be detected by DXMS and are indicated by the orange dashed lines. A) The amino-terminal portion of α5 contains 5 available hydrogens, 4 of which are forming hydrogen bonds. We observe 3-4 hydrogens exchanging for deuterium in this region. B) The β1-strand contains 6 available hydrogens, 5 of which form hydrogen bonds. DXMS analyses indicates an exchange of 4-5 hydrogens in the β1-strand.

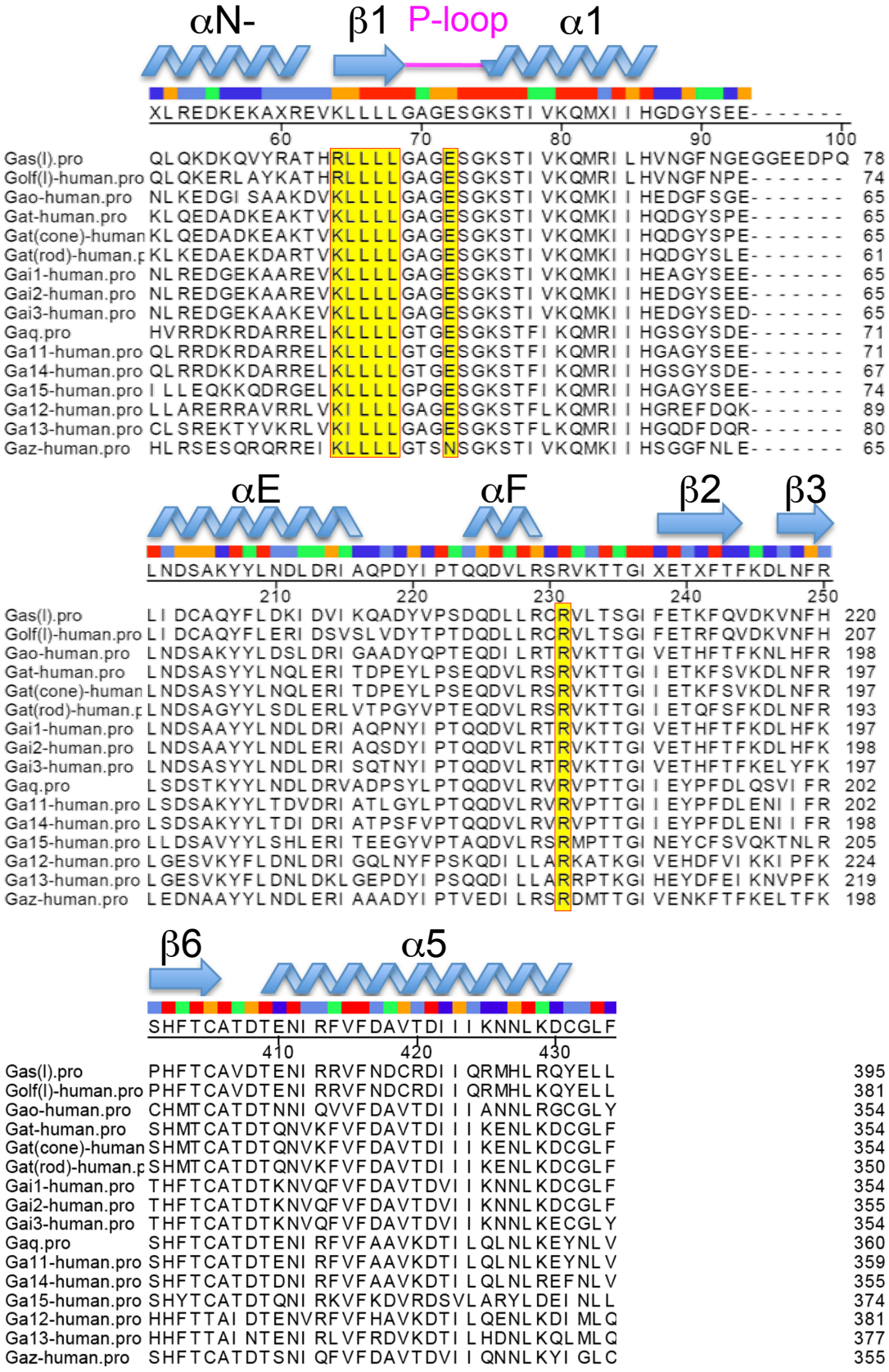

Figure S12

Figure S12

Amino acid sequence alignment of human Gα-subunits. Sequences were aligned using Lasergene (DNAStar, Madison WI) based on the Clustal W algorithm. Secondary structure is illustrated above the consensus sequence. Residues referred to in the manuscript are highlighted in yellow: the highly conserved β1-strand containing 'RLLL' motif, the conserved glutamate in the P-loop (E50 in Gαs), and conserved catalytic arginine residue (R201 in Gαs).

References

1 Kobilka, B. K. Amino and carboxyl terminal modifications to facilitate the production and purification of a G protein-coupled receptor. *Anal Biochem* **231**, 269-271 (1995).

2 Rasmussen, S. G. *et al.* Crystal structure of the beta(2) adrenergic receptor-Gs protein complex. *Nature*, doi:nature10361 [pii]
10.1038/nature10361.

3 Mendillo, M. L. *et al.* A conserved MutS homolog connector domain interface interacts with MutL homologs. *Proc Natl Acad Sci U S A* **106**, 22223-22228, doi:0912250106 [pii]
10.1073/pnas.0912250106 (2009).

4 Chen, H. *et al.* Allosteric inhibition of complement function by a staphylococcal immune evasion protein. *Proc Natl Acad Sci U S A* **107**, 17621-17626, doi:1003750107 [pii]
10.1073/pnas.1003750107.

5 Li, S. *et al.* Mechanism of Intracellular cAMP Sensor Epac2 Activation: camp-induced conformational changes identified by amide hydrogen/deuterium exchange mass spectrometry (DXMS). *J Biol Chem* **286**, 17889-17897, doi:M111.224535 [pii]
10.1074/jbc.M111.224535.

6 Sunahara, R. K., Tesmer, J. J., Gilman, A. G. & Sprang, S. R. Crystal structure of the adenylyl cyclase activator Gsalpha. *Science* **278**, 1943-1947 (1997).